Proceedings of IMECE2002
ASME International Mechanical Engineering Congress & Exposition
November 17–22, 2002, New Orleans, Louisiana

IMECE2002-39368

DEPOSITION OF YSZ THIN FILMS BY LIQUID FUEL COMBUSTION CHEMICAL VAPOR DEPOSITION

Zhigang Xu[1]
[1]NSF Center for Advanced Materials and Smart Structures (CAMSS)
North Carolina A&T State University
Greensboro, North Carolina 27411, USA
Tel: (336) 256-2511x2104
Fax: (336) 256-1153
E-mail: zhigang@camss.ncat.edu

Jag Sankar[1]
[1]NSF Center for Advanced Materials and Smart Structures (CAMSS)
North Carolina A&T State University
Greensboro, North Carolina 27411, USA
Tel: (336) 256-2511x2282
Fax: (336) 256-1153
E-mail: sankar@ncat.edu

Qiuming Wei[1,2]
[2]Center for Advanced Metallic Materials and Ceramic Systems (CAMCS)
The Johns Hopkins University
Baltimore, Maryland 21218, USA
Tel: (410) 516-5162
E-mail: qwei@pegasus.me.jhu.edu

Jim Lua
Engineering & Information Technology Group
Anteon Corporation
240 Oral School Road
Mysttic, Connecticut 06355, USA
Tel: (860) 572-9600x277
Fax: (860) 572-7328
E-mail: jlua@anteon.com

Sergey Yamolenko[1]
[1]NSF Center for Advanced Materials and Smart Structures (CAMSS)
North Carolina A&T State University
Greensboro, North Carolina 27411, USA
Tel: (336) 256-2511x2103
Fax: (336) 256-1153
E-mail: sergey@camss.ncat.edu

Devdas Pai[1]
[1]NSF Center for Advanced Materials and Smart Structures (CAMSS)
North Carolina A&T State University
Greensboro, North Carolina 27411, USA
Tel: (336) 334-7620x316
Fax: (336) 334-7147
E-mail: pai@ncat.edu

ABSTRACT

Thin film of YSZ electrolyte is highly desired to reduce the electrical resistance in SOFCs. YSZ thin Films have been successfully produced using liquid fuel combustion chemical vapor deposition (CCVD) technique. Nucleation of the YSZ particles were investigated based on two processing parameters, i.e., substrate temperature and total-metal-concentration in the liquid fuel. An optimum substrate temperature was found for highest the nucleation density. The nucleation density was increased with the total-metal-concentration. Microstructure evolution of the YSZ particles in the early stage in film growth was also studied. It was found that the particle growth rate was linear with processing time, and the particle orientation was varying with the time in the early stage of the film processing. To enhance the film growth rate, the effect of thermophoresis was studied. By increase the temperature gradient towards substrate, the effect of thermophoresis was enhanced and the film growth is also increased.

KEYWORDS

yttria stabilized zirconia, electrolyte, solid oxide fuel cell, combustion chemical vapor deposition

INTRODUCTION

Yttria fully stabilized zirconia (YSZ) is an oxygen ion conductive material and has been conventionally used as an

electrolyte in solid oxide fuel cell (SOFC) [1]. YSZ has been also used as electrolyte in oxygen sensors for pollution and safety monitoring, control and automation of industrial processes and energy conservation [2]. The electrolyte layer is placed between a cathode (air electrode) layer and an anode (fuel electrode) layer. Because of the relatively low electrical conductivity of the YSZ material (about 0.1 $S \cdot cm^{-1}$ at), most of the ohmic loss is due to the resistance of the electrolyte. To reduce the ohmic loss and increase the power generating efficiency of the fuel cell, if is desirable to use thin film electrolyte. On the other hand, temperature as high as 1000 °C is usually employed in order to obtain a reasonable ion conductivity for YSZ material. This high temperature places a great difficulty on material selection and increases the product cost greatly. Reducing the thickness of the electrolyte will increase the conductivity at lower temperatures [3].

The current techniques employed in industry for YSZ electrolyte preparation are mainly slurry spraying, slurry dipping, tape casting and screen-printing. They are simple, low-cost, and efficient techniques for industrial applications. Routine steps usually consist of iterations of coating and drying. The final product needs to be fired at high temperatures (1300-1500 °C). However, there are two common problems with these techniques. One of the problem is the difficulty to produce YSZ layers with thickness less than 500 μm with these techniques so that there will be large electrical losses in SOFC operation and the its working efficiency will be lowered. Another problem is cracks in YSZ thin layer. Moreover, the YSZ layers are usually with insufficient density (> 92-93 % of the theoretical density [1] is required for fuel cell applications). Before the problems are resolved, these techniques cannot be used in commercialization of SOFCs. YSZ thick films (normally 0.1-1 mm thick) are deposited by plasma spraying [4] which results in a porous coating with cohesion and substrate adherence problems.

Sol-gel technique is one of the methods to synthesize YSZ thin films. It was reported to require ten iterations of coating and firing at 1200°C to produce a 1.3 μm thick, smooth, dense polycrystalline coating [5]. Higher quality coatings required a 1300°C to 1400°C firing to form a 150 nm thick, epitaxial, partially stabilized YSZ layer on a single crystal fully stabilized YSZ substrate [6]. High-quality YSZ films have been deposited using metal-organic CVD (MOCVD). Both hot-wall [7,10] and cold-wall [11] reactors were used to perform the MOCVD. MOCVD of YSZ thin films was also performed with plasma-assisted CVD technique [12]. YSZ dense films have been deposited onto porous substrates using a combined technique of CVD and electrochemical vapor deposition (EVD) processes [13,14] for potential fuel cell applications.

To sum it up, among the above thin film processing techniques, the MOCVD and CVD/EVD techniques usually work in vacuum reactor, which will limit the shape and size of the part to be processed. Although Sol-gel method can be carried out in open ambient, its low productivity may limit its application in industry of SOFC manufacturing.

There is a promising technique, which is named liquid fuel combustion chemical vapor deposition (CCVD), to produce YSZ thin films for industrial purposes. Flame assisted chemical vapor deposition has long been used in industry for powder production. The vapor of metal-containing reagents is combusted in either premixed or diffusion flames of gas fuels. This method is mainly used to produce metal oxide powders [15]. The oxides are nucleated in gas phase. The particles are grown up by aggregation, agglomeration, and surface growth. The particles are collected in the downstream of the flame. The liquid fuel CCVD was first reported by Hunter et al. [16]. Metal-organic reagents were dissolved in organic solvent (toluene). The solution was atomized into small sized aerosols with a nebulizer when it was mixed with oxygen. The aerosols were ignited by a pilot flame. Thin films of Al_2O_3, SiO_2, CeO_2 and YSZ were deposited in sapphire substrates. The authors recommended that substrate needs to be placed at or beyond the end of the flame of the aerosols. The CCVD works in open atmosphere. There is potential to have conformal deposition of films on non-flat surface. Moreover, because there is no any vacuum chamber needed for the process, there will be no size limitation of the part on which the film is deposited. Because of the relatively high precursor concentration in liquid fuel to that usually used for low-pressure CVD processes, CCVD is expected to have higher deposition rate. Therefore, CCVD will be a promise technique to produce YSZ thin films for industrial SOFC applications with lower cost than any other CVD/EVD techniques.

CCVD was also studied in our research center to deposit YSZ thin films in various substrate materials, such as MgO(100), Si(100), YSZ(100), etc [17]. The chemistry in the flame was analyzes with a chemical reaction equilibrium software. The main process-controlling parameters were studied to optimize the deposition condition for high quality YSZ thin films. In this paper, results of nucleation, film microstructure evolution will be presented. The emphases of the researches were to understand the effects of lattice misfit, substrate material, and various processing parameters on the nucleation and growth. The methods to enhance the nucleation density were studied. Study on thermophoresis effect on film deposition rate and quality will also be discussed in this paper.

NOMENCLATURE

CVD: chemical vapor deposition
CCVD: combustion chemical vapor deposition
EVD: electrochemical vapor deposition
MOCVD: metalorganic chemical vapor deposition
SEM: scanning electron microscopy
SOFC: solid oxide fuel cell
TEM: transmission electron microscopy
XRD: x-ray diffraction
YSZ: yttria stabilized zirconia

EXPERIMENTAL DETAILS

The liquid fuel CCVD system had been introduced elsewhere. The system mainly consists of a quaternary high performance liquid chromatography, a nebulizer, an oxygen-methane pilot flame and the substrate heating/cooling support. Zirconium 2-ethylhexanoate (Zr-2EH) (assay 96+%, Alfa basis), Alfa Aesar) and Yttrium 2-ethylhexanoate (Y-2EH) (99.8% (metal basis) Alfa Aesar), were chosen as reagents, which were dissolved in toluene (HPLC grade, assay 99.8%, Fisher Scientific), separately. The solutions were delivered by the HPLC pump to the nebulizer with a precise flow control. The solutions were pumped into the capillary tube inside the nebulizer, while the oxidant gas flowed in the outer annular

tube of the nebulizer. At the exit of the nebulizer, aerosol of the mixture of the solutions and high-speed oxidant flow was produced. The aerosol was ignited by the pilot flame. As a result, film deposition took place on the substrate that was placed in the downstream of the aerosol flame.

The ranges and values of the parameters employed in the experiments were designed as shown in Table 1.

Table 1. Experimental parameter design

Parameter	Ranger or value
Total flow rate of solution (cm^3/min)	2.0
Flow rate of oxygen (cm^3/min)	1600
Substrate temperature (°C)	800~1200
Total-metal-concentration (M)	5.00×10^{-4} 1.25×10^{-3} 3.00×10^{-3} 5.00×10^{-3} 1.05×10^{-2}
Ratio of Yttria/Zirconia (mol%)	10
Substrate-to-nuzzle distance (mm)	76
Nucleation time (sec)	130

Most of the nucleation experiments were conducted on mirror-polished Si(100) single-crystal wafer. The wafer was cut into substrates with size of 10mm × 10mm square. Some of the experiments were carried out on MgO(100) and YSZ(100) substrates of size 5mm×10mm. The variables in nucleation studies were substrate temperature and total-metal-concentration. The effects of these two variables were conducted in two experimental groups. The nucleation densities were calculated based on the numbers of particles in a specific area on scanning electron microscopy (SEM) images obtained with the image analysis software (Image Pro Plus 4.5, Media Cybernetics, Inc.).

To observe the structural evolution of the thin films, a serial of experiments of deposition of different lengths of time had been conducted at the substrate temperature of 1200 °C, the total-metal-concentration of 1.25×10^{-3} M, on Si(100) substrates. The deposition times were 70, 130, 190, 250, 310, 370, 430, 490, 550, 610, and 670 sec.

The effect of thermophoresis on film growth was investigated by vary the substrate-to-nozzle distance and keep the substrate temperature unchanged. The effect was examined by monitoring the change of the film's thickness with the distance. Because at the smaller distances, the flame temperature became higher, leading to larger temperature gradient towards the substrate when the substrate temperature was kept unchanged.

The procedures in the film processing are briefly summarized as follows. Each substrate is cleaned by acetone and methanol ultrasonically and rinsed by de-ionized water before the deposition. Then it is properly mounted on the substrate support. With the adjusted aerosol flame of the pure toluene and the oxygen, align the substrate with the flame for the designed parameters and adjust the cooling/heating effect to the substrate to obtain the desired substrate temperature. The temperature of the substrate is measured with an infrared thermometer (OS3708, Omega Engineering, Inc.). The solutions with the reagents are then pumped into the nebulizer. The deposition is timed form this point. Except for the nucleation, the deposition time for all the samples is set for 20 min.

The morphology of all the films was characterized with SEM (Hitachi S-3000N), with some of the films characterized with transmission electron microscopy (TEM) (Philips EM300) and x-ray diffraction (XRD).

RESULTS AND DISCUSSIONS

Nucleation

It is well acknowledged that to produce smooth and dense thin films, high nucleation density is highly desired. In chemical vapor deposition, the initial step of the nucleation is the impingement of vapor molecules or precursor species on the substrate. After impingement, the vapor species can either absorb and stick permanently to the substrate, or bounce off the substrate. Even the absorbed molecules can re-evaporate in a finite time [18]. Only those molecules that equilibrate rapidly enough with the substrate will become absorbed. By diffusion of the absorbed molecules on the substrate and by incorporation of more impinging molecules from the vapor phase, larger and stable nuclei with certain number of molecules will be formed on the substrate. Substrate temperature is one of the important factors that affect the re-evaporating rate of the absorbed molecules. It was generally found that the nucleation rate decreases with increasing substrate temperature [19]. However, the dependence of the nucleation rate on the substrate temperature was dependent on the deposition system. In our experiments, the nucleation was performed at the substrate temperatures of 800 °C, 900 °C, 1000 °C, 1100 °C and 1200 °C respectively. The as-grown samples were characterized with SEM as show in Fig. 1. By counting the particle number in the specific area by the application software, it was found that the nucleation rates ranged from the order of magnitude of 10^{10} to 10^{11} cm^{-2} in the tested temperature range. The nucleation rate variation versus the substrate temperature is illustrated in Fig. 2. . It is obviously noticed that the tendency of the nucleation rate versus the substrate temperature can be divided into two sections. With the substrate temperature between 1000 °C and 1200 °C, the nucleation rate decreases with the substrate temperature, while in the substrate temperature range of 800 °C to 1000 °C, the nucleation rate increases with the substrate temperature. The former nucleation rate tendency was well accepted. As far as the author knows, the latter tendency has not been reported. It is proposed that at low substrate temperatures, the material species in the gas phase condense into the solid phase and coagulate into particles. They rebound from the surface instead of becoming adsorbed when they hit the substrate surface. This process also leads to depletion of species in the gas phase that is needed for CVD and then partially results in a decreasing of the nucleation rate. The images in Fig. 1 also reveal that on the samples nucleated at the low temperatures, there are many large nodular particles that support the above statement.

Another method to enhance the nucleation rate was to increase to deposition flux, i.e. total-metal-concentration for our experimental system. Fig. 3 shows the images of the nucleated samples with the nucleation time of 130 seconds. At the two lowest concentrations, only isolated particles presented on the substrate surface, whereas almost continuous films were

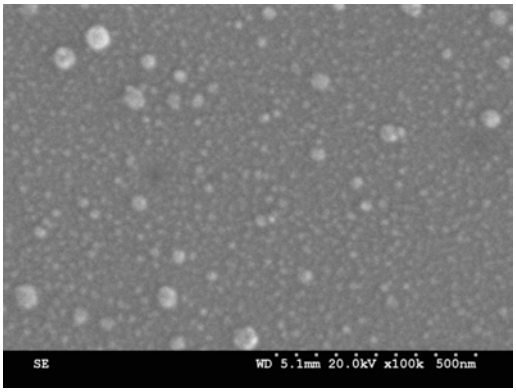

(a)

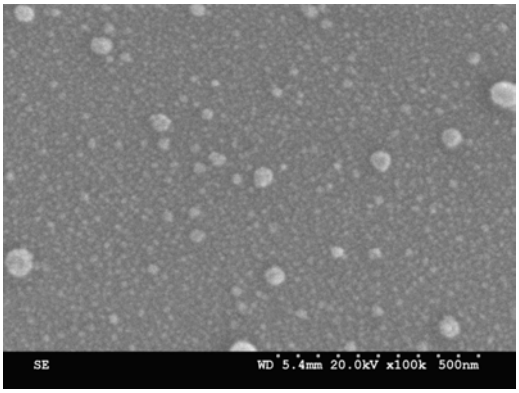

(b)

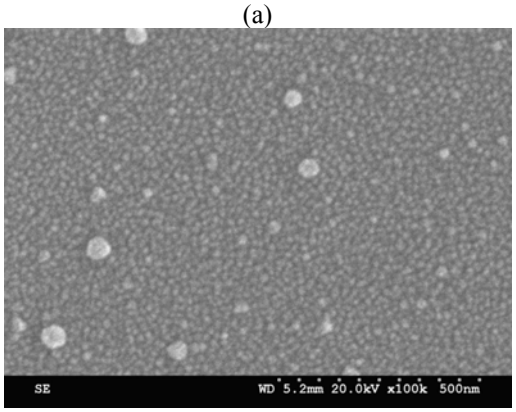

(c)

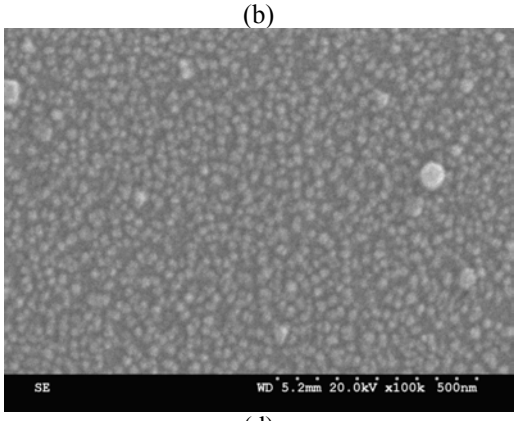

(d)

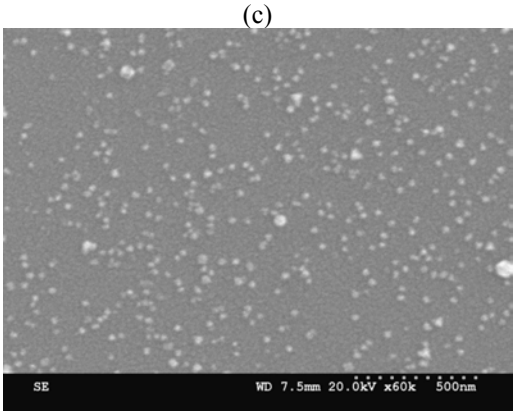

(e)

Figure 1. SEM images of YSZ nucleation processed at temperatures about (a) 800°C, (b) 900°C, (c) 1000°C, (d) 1100°C, and (e) 1200°C.

obtained when the concentration was increased to 3×10^{-3} M and up. At the large total-metal-concentrations, the particle size reached as large as 30-50 nm. From this set of experiments, it can be concluded that the lowest total-metal-concentration, 5.5×10^{-4} M, is not suitable if a high nucleation rate is demanded.

Experiments were also performed on different substrate materials. The morphologies of the nucleated crystallites on SiO_2/Si(100) and MgO(100) and YSZ(100) substrates are shown and compared in Fig. 4. On SiO_2/Si(100) substrate, nuclei are the small particles with the predominant orientation of (111) because the SiO_2 are amorphous. On MgO(100) substrate, the particles are much larger. They cover most of the substrate surface with flat-featured particles. The lattice mismatch between YSZ and MgO is within 9 % and they have the same crystal structure. Domain-epitaxial growth of YSZ on MgO is possible. At the nucleation temperature of about 1200 °C, epitaxial growth of the YSZ thin film on the YSZ(100) substrate is practical. The visible YSZ crystallites on the YSZ(100) substrate have (100) faceted square flat faces. Their edges are roughly parallel and must be aligned with the lattice matrix of the substrate.

Microstructure evolution of YSZ thin films

The evolution of thin films on substrate consists of several processes, nucleation, coarsening, coalescence, and grain growth. Coarsening is one of the ways in which the average size of islands increases. This occurs through the detachment of atoms from some islands and the diffusion of the atoms on the substrate surface to attach to other islands, resulting in the shrinkage and disappearance of some islands and the growth of other islands. Coalescence takes place when two or more islands grow to the point of contact. This happens without diffusion processes.

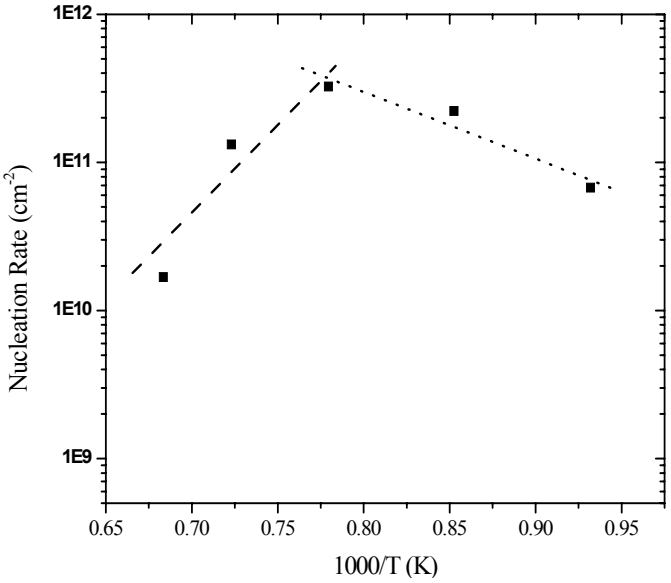

Figure 2. Nucleation rate versus substrate temperature

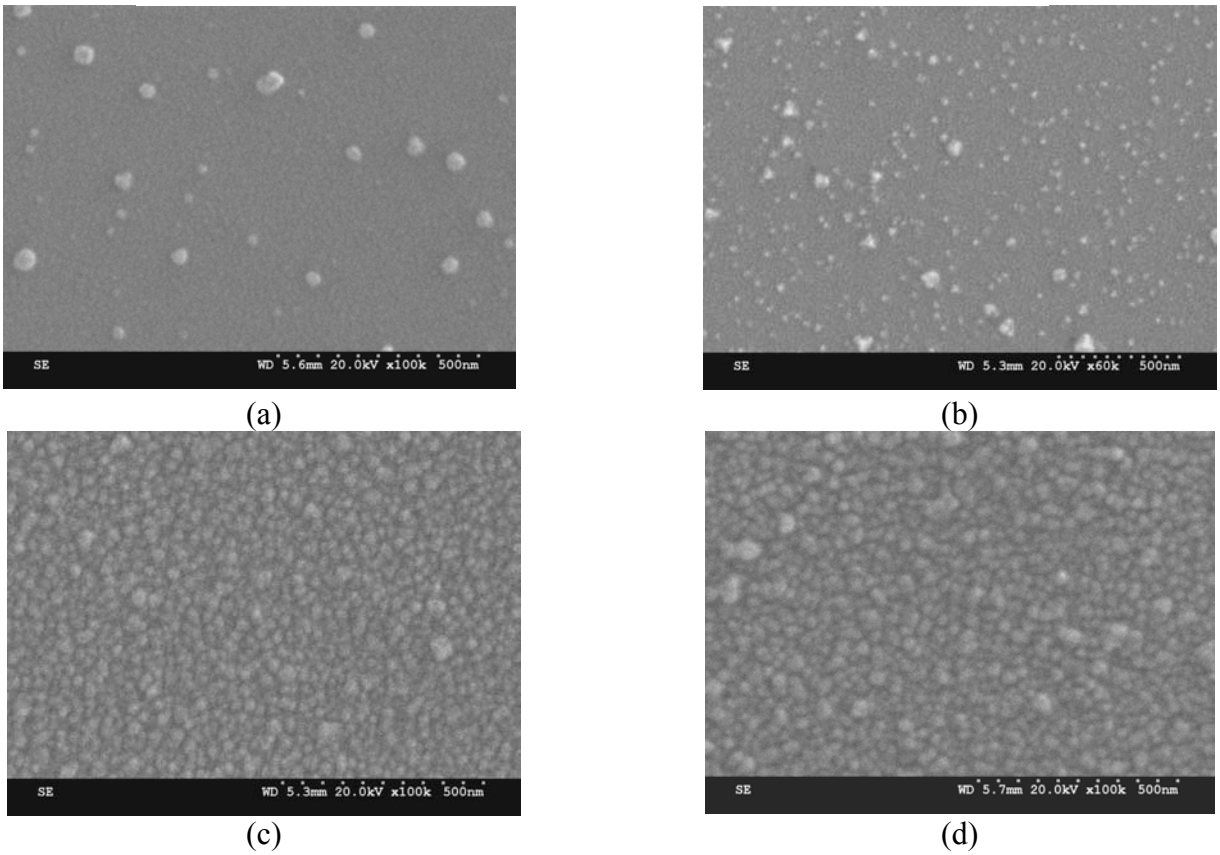

Figure 3. SEM images of the nucleated sample at different levels of total-metal-concentration, (a) 5.5×10^{-4} M, (b) 1.25×10^{-3} M, (c) 3×10^{-3} M, (d) 5.5×10^{-3} M, (e) 8×10^{-3} M, and (f) 1.05×10^{-2} M at about 1200 °C

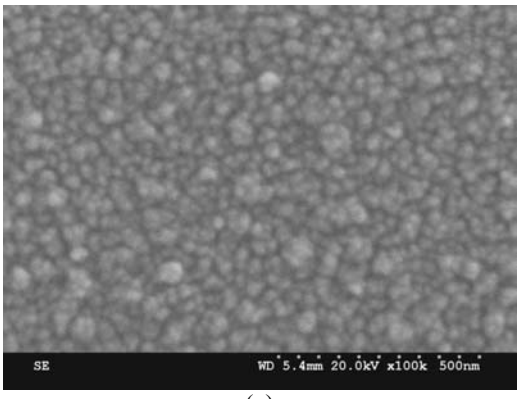

(e)

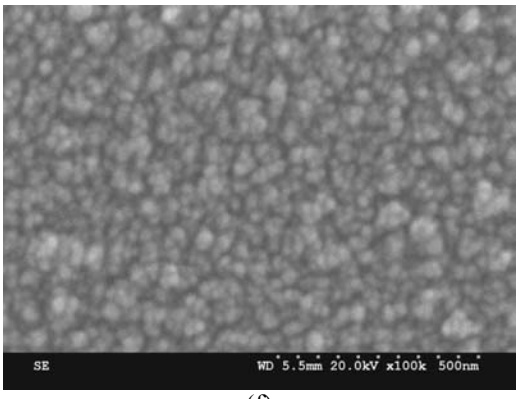

(f)

Figure 3. Continued.

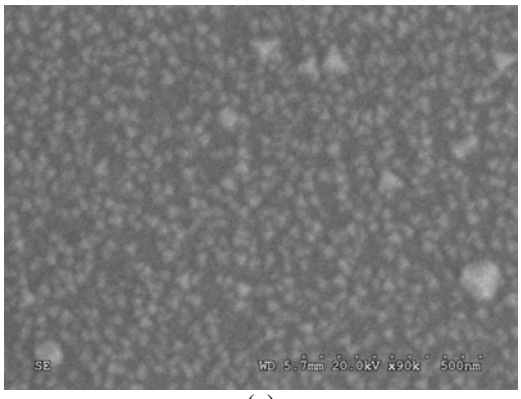

(a)

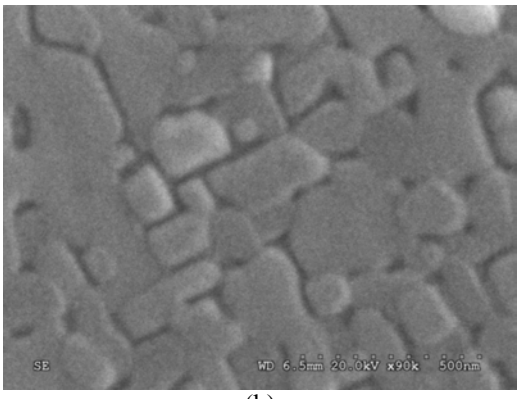

(b)

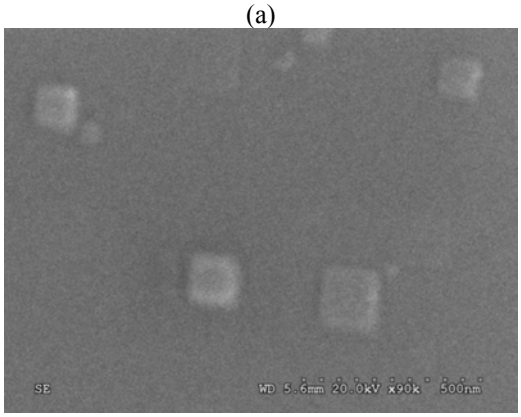

(c)

Figure 4. Morphologies of nucleated YSZ crystallites on substrates (a) SiO_2/Si(100), (b) MgO(100), and (c) YSZ(100)

The as-deposited microstructures were characterized with SEM. In Fig. 5(a), the nuclei can be hardly seen after only 70 second processing except for some large particles, which are assumed to be a result of contamination. From Fig. 5(b) to (h), with the increase in processing time, the size of the particles is increased; however, the number of the particles is reduced. This phenomenon can be interpreted by the mechanisms of coarsening and coalescence of the growing particles. When the processing time reaches 550 sec, shown in Fig. 5(i), the film is almost continuous. With the increased time of processing, the size of the particles increases. Some secondary nucleation and growth on the large particles can be noticed. It is also reasonable to assume that the secondary nucleation should take place on the substrate before all the surface of the substrate is covered with particles. The film consists of both (111) and (100) oriented crystals. In the very early stage of crystal growing, the orientation was not appreciable. When the crystallites were grown large enough in Fig. 5(d), it can be

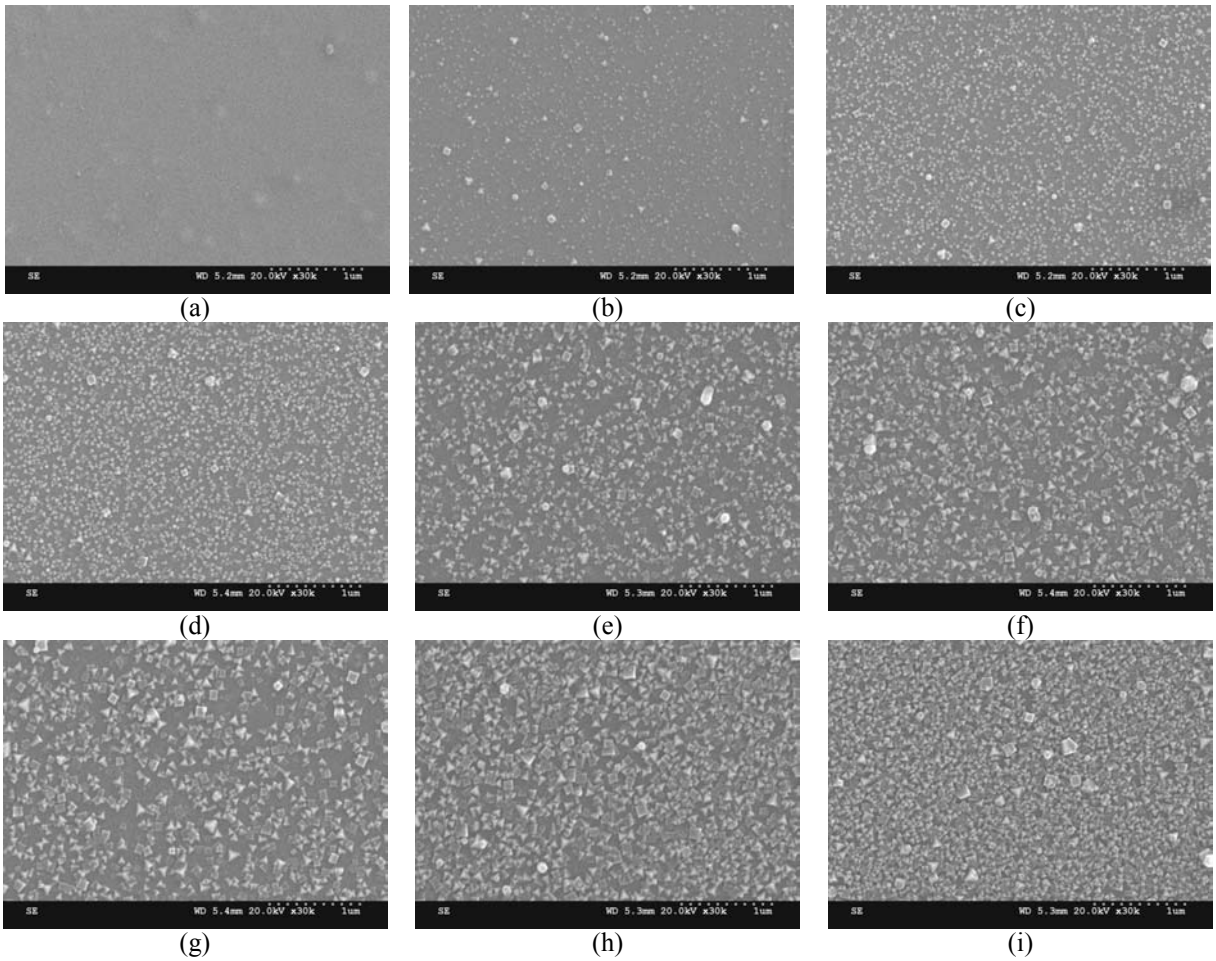

Figure 5. Microstructure of the YSZ particles/crystallites at different processing times (a) 70 sec., (b) 130 sec., (c) 190 sec., (d) 250 sec., (e) 310 sec., (f) 370 sec., (g) 430sec., (h) 490, and (i) 550 sec., at the substrate temperature of about 1200 °C

observed that the predominant orientation is (111). Until the growth was continued to 490 seconds, the image shown in Fig. 5(g) indicates that the predominant orientation becomes (100). Nevertheless, when the film grew to be almost continuous, the predominant orientation went back to (111). This could be an indication that the relative values of the energies changed with crystal growth.

According to the obtained mean particle radii, particle growth rate can be estimated by plotting the mean diameter versus the growing time as shown in Fig. 6. The particle growth rate is approximately linear during the time period studied (130 sec to 430 sec). The intercept of the line on the time axis is about 33.3 sec, which shows the incubation time for nucleation.

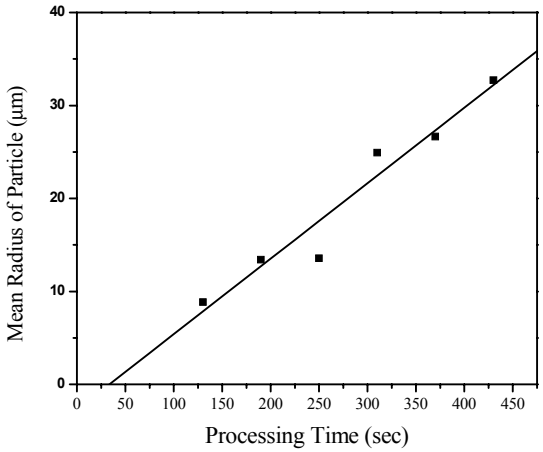

Figure 6. Particle growth rate vs. processing time

Thermophoresis Effect

Thermophoresis is the thermal gradient directed flow of material larger than vapor phase from high temperature regions to low temperature regions. Thermophoresis had been found to be a strong factor in some CVD environments [20]. A temperature gradient across a diffusion boundary layer causes

a thermophoresis effect. In our case, if the flame were hotter than the substrate, on average, the gas molecules from the substrate would have a smaller velocity than the gas molecules traveling toward the substrate. This creates a driving force for YSZ clusters formed in the direction toward the substrate. Stable gas species would not stick to the substrate, but any species that might be capable of sticking to the substrate would have a net flux to the substrate. A larger temperature gradient adjacent to the substrate increases the thermophoresis effect. The study of the effect of thermophoresis was carried out by film depositions at different substrate-to-nuzzle distances from 51 mm (far into the flame) to 83mm (out of the visible end of the flame). The film thickness measured on SEM images is plotted versus the substrate-to-nozzle distance in Fig. 7 in solid line. The data can be fitted by an exponential equation. With the increase of the substrate-to-nozzle distance,

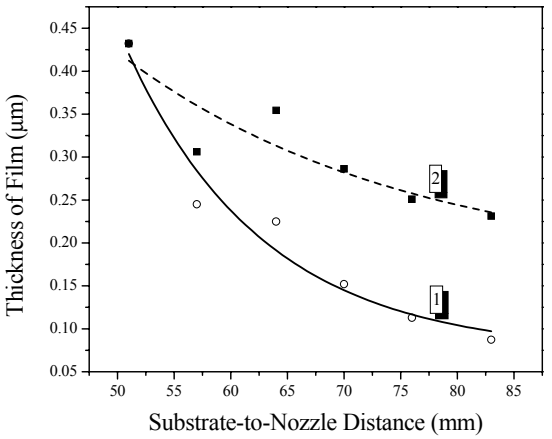

Figure 7. Film thickness as a function of the substrate-to-nozzle distance, line (1) for the original measured data, line (2) for the normalized data

precursor concentration in the flame will be attenuated because of the expansion of the flame. Normalization was made in order to eliminate the effect of concentration dilution on the film growth rate. An approximation was made by assuming that the precursor concentration at points on the axis of the flame is inversely proportional to the cross-section area of the flame at the corresponding points. According to observations, the expending angle of flame used in the experiment was about 12 degrees. Consequently, the film thickness was normalized with the cross-section area of the flame at each position that the film was deposited. The normalized thickness data were again plotted in the same graph of the originally measured data, as is shown in Fig. 6 by the curve 2 in dashed line. It is apparently noticeable that after normalization, the growth rate of the film still follows the exponentially decaying mode with the substrate-to-nozzle distance. In other words, the parameter substrate-to-nozzle distance does play a role in film growth.

From the point of view of thermophoresis, the difference in film grown rate can be interpreted as follows. When the substrate-to-nozzle distance is 83 mm, the flame temperature may be even lower or close to the substrate temperature 1200 °C, a very low film growth rate becomes understandable. By contrast, the temperature of a free flame at a distance of 51 mm from the nozzle was about 1600 °C. When the substrate is forced to be at 1200 °C, there will be a large temperature gradient near the substrate surface. The high net flux of material species will result in a high deposition rate. The change in thermophoresis effect could, in part, account for the difference in the deposition rates. However, the high deposition rate may be responsible for deteriorating the crystallinity of the film.

CONCLUSIONS

The nucleation study had shown that at low and high substrate temperatures, the nucleation was not efficient; the maximum nucleation rate could be obtained at the substrate temperature of about 1000 °C for our system. On the other hand, the morphology of the nucleated particles was influenced by the substrate material. The growth rate of the particles in the early stage before they met each other could be expressed by a linear mode. The orientation change along with deposition time was also noticed.

The effect of thermophoresis was observed in the experiments of film depositions at various substrate-to-nozzle distances, i.e., various temperature gradient between the substrate and flame near the substrate. This effect can be utilized to enhance the film growth rate. This is one of the ways to improve the productivity of the YSZ film and lower the manufacturing cost of SOFC.

ACKNOWLEDGMENTS

This research was partially sponsored by NSF through the NSF Center for Advanced Materials and Smart Structures (NSF-CAMSS).

REFERENCES

1. Blomen, L.J.M.J., and Mugerwa, M.N., 1993, *Fuel Cell Systems*, Plemun Press, New York.

2. Cawley, J.D., and Lee, W.E., 1994, "Materials Science and Technology, A Comprehensive Treatment", Chapter 2, Edited by R.W. Cahn, p. Haasen and E.J. Kramer, Volume Editor M. Swain, Vol. 11, VCH Publishers Inc., New York.

3. Will, J., Mitterdorfer, A., Kleinlogel, C., Perednis, D., and Gauckler, 2000, "Fabrication of thin electrolyte for second-generation solid oxide fuel cells", Solid Oxide Ionics, **131**, pp.79-96.

4. Varacalle, D.J. Jr., et al., 1989, "Plasma sparying of zirconia coatings", Mat. Res. Symp. Proc., Vol. 155, pp.235-246.

5. Chihiro, C., Fukui, T. and Okuyama, M., J. 1993, "Prearation of zirconia coatings by hydrolysis of zirconium alkoxide with hydrogen peroxide", Amer. Ceram. Soc., **76**(4), pp.1061-1064.

6. Seifert, A., Lange, F. F., and Speck, J. S., 1993, "Liquid precursor route for hetero-epitaxy of $Zr(Y)O_2$ thin films on (001) cubic zirconia", J. Amer. Ceram. Soc., **76**(2) pp.443-448.

7. Garcia, G., Casado, J., Llibre. J., and Figueras, A., 1995, "Preparation of YSZ layers by MOCVD: influence of experimental parameters on the morphology of the films", J. Crystal Growth, **156**, pp.426-432.

8. Yamane, H., and Hirai, T., 1989, "Yttria stabilized zirconia transparent films prepared by chemical vapor deposition", J. Crystal Growth, **94**(4), pp. 880-884.

9. Akiyama, Y., Sato, T., and Imaishi, N., 1995, "Reaction analysis for ZrO_2 and Y_2O_3 thin film growth by low-pressure metalorganic chemical vapor deposition using β-diketonate complexes", J. Crystal Growth, **147**, pp. 130-146.

10. Hwang, S-C. and Shin, H-S., 1999, "Effect of deposition temperature on the growth of yttria-stabilized zirconia thin films on Si(111) by chemical vapor deposition", J. Am. Ceram. Soc., **82**(10), pp.2913-2915.

11. Chour, K-W., Chen, J., and Xu, R., 1997, "Metal-organic vapor deposition of YSZ electrolyte layers for solid oxide fuel cell applications", Thin Solid Films, **304**, pp.106-112.

12. Holzschuh, H., and Suhr. H., 1992, "Plasma-Enhanced CVD of Yttria Stabilized Zirconia", High T_c Superconductor Thin Films , pp.653-658.

13. de Haart, L.G.J.; Lin, Y.S.; de Vries, K.J.; Burggraaf, A.J.; 1991, "Modified CVD of nanoscale structures in and EVD of thin layers on porous ceramic membranes", J. Eur. Ceram. Soc., **8**(1), pp. 59-70.

14. Suzhki, M., Sasaki, H., Otashi, S., Kajimura, A., Sugiura, N., and Ippommatsu, M., (1994), "High performance solid oxide fuel cell cathode fabricated by electrochemical vapor deposition", J. Electrochem. Soc. **141**(7), pp.1928-1931.

15. Pratsinis, S.E., 1998, "Flame aerosol synthesis of ceramic powders", Prog. Energy Combust. Sci. **24**, pp.197-218.

16. Hunt, A.T., Carter, W.B., and Cochran, J.K., Jr., 1993, "combustion chemical vapor deposition: A novel thin-film deposition technique", Appl. Phys. Letts. **63**(2), pp. 266- 268.

17. Xu, Z., Sankar, J., and Wei, Q., 2001, "Combustion chemical vapor deposition of YSZ thin films for fuel cell applications", Proc. Of 2001 ASME Intel. Mech. Eng. Cong. and Exp., CD-ROM version.

18. Neugebauer, C.A., 1970, *Handbook of Thin Film Technology*, ed. Maissel, L.I., Glang, R., Chapter. 8, New York, McGraw-Hill.

19. Thompson, C.V., 2000, "Structure elvotion during processing of polycrystalline films", In *Annu. Rev. Mater. Sci.,* **30**, pp. 159-190.

20. Bai, W., Choy, K.L., Stelzer, N.H.J., and Schoonman, J., 1999, "Thermophoresis-assisted vapour phase synthesis of CeO_2 and $Ce_xY_{1-x}O_{2-\delta}$ nanoparticles", Solid State Ionics, 116, pp.225-228.